

Estimation of annual forest evapotranspiration from a coniferous plantation watershed in Japan (1): Water use components in Japanese cedar stands



Tomo'omi Kumagai^{a,*}, Makiko Tateishi^b, Yoshiyuki Miyazawa^c, Masahiro Kobayashi^d, Natsuko Yoshifuji^e, Hikaru Komatsu^f, Takanori Shimizu^d

^aHydrospheric Atmospheric Research Center, Nagoya University, Chikusa-ku, Nagoya 464-8601, Japan

^bKasuya Research Forest, Kyushu University, Sasaguri, Fukuoka 811-2415, Japan

^cResearch Institute for East Asia Environments, Kyushu University, Motoooka, Fukuoka 811-0395, Japan

^dForestry and Forest Products Research Institute, Matsunosato, Tsukuba, Ibaraki 305-8687, Japan

^eGraduate School of Agriculture, Kyoto University, Kyoto 606-8502, Japan

^fThe Hakubi Center, Kyoto University, Kyoto 606-8302, Japan

ARTICLE INFO

Article history:

Received 14 June 2013

Received in revised form 29 August 2013

Accepted 28 October 2013

Available online 5 November 2013

This manuscript was handled by Konstantine P. Georgakakos, Editor-in-Chief, with the assistance of Matthew McCabe, Associate Editor

Keywords:

Cryptomeria japonica

YPLANT

Evapotranspiration

Slope position

Hillslope aspect

Error

SUMMARY

To increase the ability to control forest ecosystem water and carbon cycles using forest management, we estimated watershed-scale evapotranspiration (ET) and its components, i.e., upper-canopy stand transpiration (E_{UC}), sub-canopy vegetation transpiration (E_{SC}), and canopy interception (I_C), in a Japanese cedar (*Cryptomeria japonica* D. Don.) plantation over a whole year. For E_{UC} , xylem sap flux density was measured in three plots: an upper (UP) and lower (LP) plot on a northeast-facing, and one on a south-facing slope (SP). Mean stand sap flux density (J_S) in the UP, LP, and SP was similar despite differences among plots in tree density and size, implying that J_S measured in a partial stand within the watershed is a reasonable estimator of the values of other stands, and that stand sapwood area is a strong determinant of the E_{UC} . Prior information on annual variations in ET and its components was insufficient and urgently needed in Japan. Using a combination of observations and modeling, we obtained reliable estimations of E_{SC} and I_C , and thus, of annual variations in ET and its components (911.4, 359.3, 126.9, and 425.2 mm/year for ET , E_{UC} , E_{SC} and I_C , respectively). We found a conservative ratio of I_C to rainfall (P) (I_C/P) throughout the year, a significant contribution of I_C/P to the ratio of ET to P (ET/P) during heavy rainfall conditions, and an increase in I_C and E_{SC} when E_{UC} was decreasing, resulting in a constant monthly ET/P in the growing season and winter. These support the idea of the conservative process of forest water use in that P mainly controls ET on a monthly and longer time scale.

© 2013 Elsevier B.V. All rights reserved.

1. Introduction

Forests cover 66% of the total land area in Japan, with plantation forests constituting 41% of the forested area. This is a result of extensive reforestation following deforestation in World War II. Forty-three percent of Japan's plantation forest area comprises a single tree species: Japanese cedar (*Cryptomeria japonica* D. Don.) (Japan Forest Agency, 2011). Although Japanese cedar is the most popular wood material in Japan and extensive research has been conducted on its wood quality, information on the use of this species for environmental benefits is scarce (Kumagai et al., 2007, 2008). Currently, Japan imports large amounts of timber and forest

products, and environmental roles of forests are gaining precedence over that of timber production (Fujimori, 2000).

Japan has relatively little area that is level and lowland, and mountainous watersheds supply almost all of the water resources to the lowlands. The majority of the forests are situated in mountain regions, and mountains tend to receive higher precipitation (Sawano et al., 2005). On an annual basis, subtracting forest water use from precipitation denotes the upper limit of available water (see Komatsu et al., 2008b). Therefore, forest management such as thinning and forest conversions has been expected to alter forest water use components, such as upper- and sub-canopy transpiration and interception, and improve the ability of forests to control water yield, especially in plantation forests (see Komatsu et al., 2008a).

Many of the forest water use theories assume larger evaporative demand than annual precipitation (i.e., $E_{eq} \geq P$, where E_{eq} is equilibrium evaporation and P is precipitation) and an evenly

* Corresponding author. Address: Hydrospheric Atmospheric Research Center, Nagoya University, Furo-cho, Chikusa-ku, Nagoya, Aichi 464-8601, Japan. Tel.: +81 52 789 3478; fax: +81 52 788 6206.

E-mail address: tomoomikumagai@gmail.com (T. Kumagai).

distributed P throughout the year or a large P in winter (see Koma-tsu et al., 2007, 2008b). Scientists from the US and UK devised these theories for application to their familiar hydrologic environment, thus, detailed information of forest water use when $E_{eq} \ll P$ and when there is a large P in summer conditions, as in most East Asian countries, should be more important locally and globally.

The goal of this study was to obtain quantitative and process information on forest water use in a typical Japanese cedar watershed, which is also the typical forest watershed in moist East Asian regions. Questions to be addressed were: (1) how the evapotranspiration (ET) is assigned to the water use components such as overstory and understory vegetation transpiration and canopy interception; (2) what the spatial variation of ET in a watershed is; and (3) what biological and/or environmental factors determine the spatial variation (see Ford et al., 2007; Baldocchi and Ryu, 2011). These are especially important in hilly regions of Japan, where topographical gradients have a strong influence on plant-soil systems. To achieve this goal, we conducted stand-level sap flow measurements at different elevations on northeast- and south-facing slopes, and combined canopy interception measurements and their model estimates using biometric data from several plots, and model estimates of transpiration from sub-canopy vegetation using individual-leaf level ecophysiological traits; further, we examined the observation strategies for estimating forest water use at our study site. Finally, we validated forest water use estimated in this study using eddy covariance water vapor flux and catchment water balance measurements at this site, and reported in earlier publications in Japan (see Komatsu et al., 2008b).

2. Materials and methods

2.1. Study site and meteorological measurements

The experiments were carried out in the Kahoku Experimental Watershed (KHEW), a 2.63 ha evergreen coniferous plantation on the island of Kyushu, Japan (33°08'N, 130°43'E, 150–220 m a.s.l.). The watershed is underlain by crystalline schist and the slopes on both sides of the valley are steep (20–40°). The mean annual precipitation for the period 2000–2008 was 2138 mm, with rainy season from mid-June to early July. The mean annual temperature was 15.3 °C with a minimum mean monthly of about 4 °C in January–February and a maximum mean monthly of about 26 °C in August.

The forest in the watershed consists mainly of even-aged 50-year-old (in 2007) *C. japonica* stands, and to a lesser degree, *Chamaecyparis obtusa* Endl. (Japanese cypress) stands ranging in age from 30 to 50 years old (in 2007). Although the planting areas of these species are almost equal, half of the Japanese cypress trees in KHEW are comparatively young and small. In $\approx 20\%$ of KHEW, broadleaf trees species compete with the planted conifers, forming a patchy forest watershed. Understory vegetation is dense and consists of various species of evergreen trees such as *Quercus glauca* Thunb., *Castanopsis sieboldii* Hatsusima ex Yamazaki et Mashiba., and *Eurya japonica* Thunb. For the sap flow measurements in this study, we sampled three plots within the Japanese cedar stand: an upper-slope plot (UP) and a lower-slope plot (LP), located less than 100 m from each other on a 20° northeast-facing slope, and a middle-slope plot on a 25° south-facing slope (SP) (see Table 1). Although the plots were of the same age, tree densities increased in the order UP > SP > LP, and the stand basal area and individual tree sizes varied in the order LP > SP > UP (Table 1). It should be noted that the frequency distributions of diameter at breast height (DBH) in the LP was different to those of the UP and SP, which were similar to each other. The silhouette area index of leaves plus stems and branches (plant area index; PAI) including that of under-

Table 1

Stand characteristics of the three study plots. UP and LP (upper and lower slope plots on a northeast-facing slope, respectively), and SP (middle slope plot on a south-facing slope).

Characteristic	UP	LP	SP
Plot area (m ²)	318	321	203
Age (years in 2007)	50	50	50
Density (trees ha ⁻¹)	1575	904	1330
PAI ^a (m ² m ⁻²)	3.2–5.4 ^b	4.4–5.7	3.6–5.9
Mean DBH (cm)	23.8	40.3	26.6
Range DBH (cm)	12.5–30.8	23.7–53.3	14.3–33.7
Basal area (m ² ha ⁻¹)	71.7	118.7	76.3
Sapwood area ^c (m ² ha ⁻¹)	36.3	46.0	37.3
Mean height (m)	22	32	22 ^b
Sap flux measurements (trees)	23	15	19

^a PAI was measured from 2004 to 2005, and ranges of values denote seasonal variations.

^b Measured at other slope positions with similar characteristics to the study plot.

^c Sapwood area was estimated for each study plot based on allometric relationships.

story vegetation was measured every month in the period 2005–2006 around three basic PAI observation points in the watershed using a plant canopy analyzer (LAI-2000, Li-Cor, Lincoln, NE). The PAI ranged from 4.4 to 5.7 m² m⁻² and from 3.6 to 5.9 m² m⁻² in the LP and SP, respectively, implying minor seasonal variation.

Micrometeorological conditions and eddy-covariance fluxes were measured at the top of the canopy using a 50-m-tall canopy tower located at the center of the watershed. Wind speeds and gas concentration time series at a height of 51 m were all sampled at 10 Hz using a three-dimensional sonic anemometer (DA600-3T, Kaijo, Tokyo, Japan) co-located with a gas-inlet leading to a closed-path CO₂/H₂O analyzer (Li-7000, Li-Cor). All variances and covariances required for eddy-covariance flux estimates were computed over a 30-min averaging interval. According to the species distribution and topography map, wind directions were categorized so that each of them could be related to the fluxes from specific vegetation surfaces. If a wind direction was out of the appropriate categorization, the fluxes were interpolated with a generic multiple imputation method (see Hui et al., 2004). Furthermore, it was assumed that the eddy fluxes were underestimated by $\approx 25\%$ (the energy imbalance ratio observed in this site) and the flux values were divided by this value. The resultant eddy water vapor flux was considered to be the whole-ecosystem ET , i.e., the total of wet and dry canopy evaporation and sub-canopy evaporation.

A solar radiometer (CM14B, Kipp & Zonen, Delft, Netherlands), a net radiometer (CNR4, Kipp & Zonen) and a ventilated psychrometer (NH020L, EKO, Tokyo, Japan) were installed at a height of 47, 50.5 and 42 m, respectively. Note that the UP and LP are on the highest and the lowest elevations in the studied plots, respectively. While the ground level is 20–30 m higher in the UP than in the LP, the canopy height in the UP is around 10 m lower than in the LP (see Table 1). In short, the canopy surfaces of all plots are somewhat even. Samples were taken every 30 s for solar radiation (R_s ; W m⁻²) and net radiation (R_n ; W m⁻²), and every 1 min for air temperature (T_a ; °C) and relative humidity (RH ; %), and averaged over 30 min intervals (CR10X, Campbell Scientific, Logan, UT). In an open field located approximately 100 m from the watershed, a tipping bucket rain gauge (RT-5, Ikeda Keiki, Tokyo, Japan) was placed on a waist-height bench. Discharges from the study watershed and a neighboring one were also measured using weirs. Further details of the experimental setup and data processing for the eddy flux and discharge are presented elsewhere (Shimizu et al., submitted for publication, hereinafter referred to as submitted manuscript, 2013).

Volumetric soil moisture content (θ ; $\text{m}^3 \text{m}^{-3}$) and matric potential (Ψ ; m) were measured in each plot at 10, 20, and 40 cm below the forest floor at 30-min intervals (CR10X). A dielectric aquameter sensor (EC-10, Decagon Devices, Inc., Pullman, WA) was used to measure the time series of θ . A tensiometer (DIK3151, Daiki, Tokyo, Japan) was used to monitor Ψ at the same depth as θ , thereby providing the necessary measurements to compute in situ θ – Ψ curves, i.e., soil water retention curves. Ψ at the inflection point and the air entry on the θ – Ψ curves indicated the distributions of soil pore sizes (see Kosugi, 1994). The weighted average of θ in the 0–50 cm soil layer was calculated as $\theta_{0-50} = (15\theta_{10} + 15\theta_{20} + 20\theta_{40})/50$ (where θ_{10} , θ_{20} and θ_{40} are θ at depths 10, 20, and 40 cm, respectively, in $\text{m}^3 \text{m}^{-3}$).

2.2. Sap flux measurements, sapwood analysis, and calculations of upper canopy stand transpiration

Xylem sap flux density (F_d) measurements were conducted using the thermal dissipation method with Granier-type sensors (e.g., Granier, 1987). Each sensor consists of a pair of probes 20 mm long and 2 mm in diameter. The probes were inserted into the sapwood approximately 0.15 m apart. The upper probe, including a heater, was supplied with 0.2 W constant power. The heat was dissipated into the sapwood and vertical sap flux surrounding the probe. The temperature difference between the upper heated probe and the lower unheated reference probe was then measured and converted to F_d after Granier (1987). Sap flow signals were scanned with a data logger (CR10X) with a multiplexer (AM16/32, Campbell Scientific) every 30 s and averaged over 30 min. For F_d measurements, 23, 15, and 19 trees were selected in the UP, LP and SP, respectively (see Table 1), so that the number of trees measured in each DBH class corresponded to the frequency distribution of DBH in those plots. One to three sensors were inserted into each selected tree at depths of 0–20, 20–40, and 40–60 mm to cover the sapwood, and 20, 10 and 11 trees were used in the UP, LP and SP, respectively, for the measurements of the radial F_d profiles. Using pooled data on tree-to-tree and radial variations in F_d and the Monte Carlo sampling technique, it was confirmed that no more than 10 trees were needed as a sample size for sap flux measurements for estimating stand transpiration in each plot (see Kumagai et al., 2007).

Sensors were positioned about 0.15 m circumferentially apart from each other at a height of about 1.3 m. For sensor access to 20–40 and 40–60 mm depths, larger holes were made in the trunk to enable installation of the sensors in deeper sapwood. Japanese cedar trees in plantations are commonly characterized by a perfectly circular stem cross-section and circumferentially constant sapwood thickness; therefore, we assumed the azimuthal variation in F_d to be small (e.g., Vertessy et al., 1997). In addition, most sensors were placed on the north-facing side of the trees to avoid sun-exposure; further, the part of the trunk into which the sensors were inserted was fully insulated to prevent any direct radiation. Although some sensors were not placed on the north-facing side because of topographical obstacles, there was only a slight natural thermal gradient (not more than 0.2 °C) along the trunks of all measured trees, likely due to the closed canopy and shade of the steep slope. Therefore, the data were not corrected for this. It is known that F_d from sensors positioned on the shaded side of tree crowns is often underestimated (e.g., Oren et al., 1999). This effect occurs when conduits are vertically straight and/or the hydraulic system on one side of a stem services one part of the tree crown. Spiral conduits generate a uniform sap flow distribution whereas straight vertical conduits follow a direct path of least resistance (see Kubler, 1991). It was demonstrated in an experiment using a dye solution (acid fuchsin) injected into a radial hole bored into the tree trunk, that the conduits in Japanese cedar are spiral and

the segmentation of the hydraulic system is weak (data not shown). Therefore it was assumed that systematic underestimation of F_d was not caused by placing sensors on the north-facing side of the tree trunks and that the azimuthal variation in F_d was included in the tree-to-tree variation in F_d . Therefore, F_d was not measured at different orientations within a tree trunk.

Sapwood thickness (in mm) of each sample tree was measured on a core extracted with a 5-mm increment borer about 1.3 m above-ground, and assessed as the mean of two orthogonal measurements. Distinct color differences were used to identify the boundary between sapwood and heartwood. Tree sapwood area (A_{S_tree}) was obtained from the difference between the stem cross-sectional area beneath the bark and heartwood area assuming that the stem cross-sections were circular. Conducting tissue in the sapwood of Japanese cedar extends from just beneath the bark to a non-conducting “white zone” at the sapwood-heartwood boundary, in which the moisture content is much lower than that of the heartwood (Nobuchi and Harada, 1983; Nakada et al., 1999). The radial position of the “white zone” can be predicted because sapwood thickness can be predicted from the relationship between DBH and individual sapwood area or thickness conducted at this study site by Kumagai et al. (2007). There is no water movement in the “white zone” (Kumagai et al., 2005) and its width was assumed to be constant at about 10 mm (data not shown). Note that the dye solution experiment confirmed our ability to identify the boundary between sapwood and heartwood and the “white zone” in the stem cross section of Japanese cedar. Therefore, precautions were taken when inserting sensors in the sapwood to ensure coverage of the hydroactive area. Also, sensors at the deepest positions of the sapwood were in contact with non-conducting wood, but errors in calibrating the Granier-type sensors were considered to be small because F_d at this position was at most 0.01 mm s^{-1} (Clearwater et al., 1999). Furthermore, the sap volume flow in the deepest xylem band is very small compared with that in the total sapwood; thus, data were not corrected.

The mean stand sap flux density (J_s) was computed as the area-weighted mean F_d for the 0–20, 20–40, and 40–60 mm xylem bands of all measured trees within each plot according to Kumagai et al. (2005, 2007). Individual-level transpiration, J_s , was scaled up to the stand level (Wilson et al., 2001; Wullschlegel et al., 2001; Schäfer et al., 2002; Pataki and Oren, 2003; Kumagai et al., 2005, 2007) using the following equation:

$$E_{UC} = J_s \frac{A_{S_stand}}{A_G}, \quad (1)$$

where E_{UC} is the upper canopy stand transpiration, and A_G is the ground area of the stand. A_{S_stand} is the total sapwood area of the stand, which was estimated from the relationship between DBH and the individual tree's sapwood area and DBH values measured for all Japanese cedar trees in the stand plot. In addition, the individual tree water use (T_i) of each tree, which was measured F_d over the entire conducting wood, was obtained as the sum of the product of F_d and the conducting area at each xylem band.

To examine whether watershed-scale E_{UC} ($E_{UC,T}$) can be derived from individual-to-plot scale sap flow measurements, the $E_{UC,T}$ was assumed to be the weighted average E_{UC} over the three studied plots, estimated as

$$E_{UC,T} = \frac{A_{G_UP}E_{UC_UP} + A_{G_LP}E_{UC_LP} + A_{G_SP}E_{UC_SP}}{A_{G_UP} + A_{G_LP} + A_{G_SP}}, \quad (2)$$

where subscripts UP, LP and SP denote the upper, lower, and the south-facing slope plots, respectively. The estimation errors caused by this assumption will be examined later.

2.3. Estimation of transpiration from sub-canopy vegetation

We estimated transpiration (E) from sub-canopy vegetation (E_{SC}) using the YPLANT model (Pearcy and Yang, 1996) with measurements of individual leaf scale physiological traits and the three-dimensional tree architecture. For this estimation, we selected three species, *Q. glauca*, *C. sieboldii*, and *E. japonica* as the main sub-canopy vegetation, and used five to seven sample saplings of each species.

It should be noted that in this study YPLANT was used to scale up E_{SC} from the leaf-level to the community-level on the premise that the leaf-level E_{SC} measurements could be well reproduced. Reconstruction of the three-dimensional structure and acquisition of leaf physiological parameters for each sample sapling are required to run YPLANT. The architectural measurements were conducted under the cypress understory at another site in Kyushu (Miyazawa and Otsuki, 2010), on the assumption that the small sapling size would approximate the architecture, light absorption, and gas exchange of the branches (modules) of the understory canopy at the study site. We first measured the direction (azimuth and zenith); then we measured the lengths and diameters of all internodes and petioles, and the surface area of all leaf blades of the saplings so that each node and the attached leaves could be correctly re-placed in the reconstructed sapling in the computer. In addition, we took hemispherical photographs above all the sample saplings with a fisheye lens (FC-E 0.21×, Nikon Corporation, Tokyo, Japan) attached to a digital camera (CoolPix 990, Nikon Corporation), and analyzed the distribution of the overstory foliage and the canopy gaps of each photograph using the HemiView Canopy Analysis software (Delta-T Devices, Cambridge, UK).

The gas exchange traits of the understory leaves were measured using a portable infrared gas analyzer (Li-6400, Li-Cor, Lincoln, NE). Gas exchange of the leaves within the cuvette was measured under light saturation and 11 steps of cuvette CO_2 concentrations to obtain the parameters required for the modeling of gas exchange rate, e.g., the photosynthetic capacity as the maximum rate of RuBP carboxylation (see Farquhar et al., 1980). The photosynthetic rate was estimated using these photosynthetic capacity parameters and environmental factors such as light and leaf temperature. The leaf-level E_{SC} was computed as a product of a leaf vapor pressure deficit and stomatal conductance as a function of the photosynthetic rate, leaf surface humidity and leaf surface CO_2 concentration (Ball–Berry type model: see Collatz et al., 1991). The Ball–Berry type model does not intrinsically consider the soil moisture deficit effects, but because we determined the model parameter, which is affected by the soil moisture condition at each observation period, the soil moisture control was resultantly incorporated into the stomatal conductance calculation. The measurements were carried out for three saplings per species and 8–10 current-year leaves per saplings in the study site. Although photosynthetic traits were known to change with leaf age (e.g., Escudero and Mediavilla, 2003), an area ratio of the older leaves was much smaller than that of current-year leaves in each sapling, and therefore, we assumed that photosynthetic traits of all the leaves were the same as that of current-year leaves.

The canopy openness analyses and the reconstructed architectural leaf arrangements enabled us to estimate light absorbed by all the leaves of each sample sapling, and as a result, we can estimate each individual sapling E using the measured leaf gas exchange capacities. The LAI of the sub-canopy vegetation was arbitrarily determined to be 2.0 from observations of leaf area density profiles, which estimated the LAI at 1.8–2.5. Assuming little seasonal change in the LAI of the sub-canopy evergreen species, the E_{SC} was produced by the LAI and the sapling E per leaf area converted from the whole-sapling E .

The community-level E_{SC} should have been investigated at several plots in the watershed so that their spatial variation can be compared with that in the E_{UC} . However, although we used a single plot, we elaborated and conducted extensive and technically difficult experiments to estimate the E_{SC} correctly.

2.4. Canopy interception measurement and model

In the studied site, three plots were instrumented for stemflow and throughfall measurements (Shimizu et al., submitted for publication). Plots 1 and 3 were established in stands of Japanese cedar; data obtained were used in the following analysis. Note that plot 1 was located in the neighboring watershed, but the size and tree density were almost the same as in the SP. In each plot, 0.40 and 0.45 m² troughs made of hard PVC were connected to 0.2-L tipping bucket flow meters (UIZ-200, Uizin, Tokyo, Japan). Collars around the trunks were connected to 0.5-L tipping bucket flow meters (500 cc-model, Yokogawa Electric Corporation, Tokyo, Japan) allowing stemflow measurements on four trees in plot 1 and two trees in plot 3 (the areas covered by sample trees were 21.4 and 45.5 m², respectively). The throughfall and stemflow measurements were sampled as the time-of-tip (one tip denotes the throughfall of 0.22 and 0.25 mm and the stemflow of 0.024 and 0.011 mm for plots 1 and 2, respectively) by event data logger (H07-002-04, Onset, MA). Rainfall losses by canopy interception (I_C) were calculated by subtracting both stand throughfall and stemflow from gross rainfall (P). The detailed tipping bucket data corrections are presented elsewhere (Iida et al., 2012; Shimizu et al., submitted for publication).

In addition, the canopy interception model originally proposed by Kondo et al. (1992) was used to validate the I_C estimates in this study. Kondo and others' model has been frequently applied to forest environments in Japan and its applicability and validity for the Japanese climate have been well confirmed (Komatsu et al., 2008c). A review and description of the canopy interception model is provided below for completeness.

Assuming that a single storm event does not exceed one day, and that multiple storm events during a day can be lumped together as a single daily storm, potential evaporation rate (E_{POT}), storm duration (τ), canopy storage of the intercepted rainwater (S), probability that raindrops strike the canopy (Ω^*) and the daily rainfall amount (P) are needed to describe the daily I_C , given by

$$I_C = \begin{cases} E_{POT} \frac{\tau}{24} + S, & \text{for } \Omega^* P \geq E_{POT} \frac{\tau}{24} + S_{max} \\ \Omega^* P, & \text{for } \Omega^* P < E_{POT} \frac{\tau}{24} + S_{max} \end{cases}, \quad (3)$$

where S_{max} is the canopy storage capacity, assumed to be 2.0 for whole the study period, which was the maximum value obtained in August (Komatsu et al., 2008c). Upper and lower equations of Eq. (3) denote canopy rainwater losses to the atmosphere when storms are larger and smaller than a threshold, i.e., the amount of rainwater needed to saturate the canopy storage, respectively. Although the original model by Kondo et al. (1992) used E_{POT} calculated by single-layer heat-budget model (Kondo and Watanabe, 1992), here, the equilibrium evaporation function of R_n as E_{POT} (see Priestley and Taylor, 1972) was used for simplicity, and τ , S , and Ω^* were, respectively, formulated as

$$\tau = 18 \left\{ 1 - \exp \left(-\frac{P}{12} \right) \right\}, \quad (4)$$

$$S = S_{max} \left\{ 1 - \exp \left(-\frac{P}{S_{max}} \right) \right\}, \quad (5)$$

and

$$\Omega^* = \Omega \left\{ 1 - \exp \left(-\frac{0.5PAI}{\Omega} \right) \right\}, \quad (6)$$

where Ω is canopy closure, assumed to be 0.9, typical value of coniferous forest in Japan (Komatsu et al., 2008c). Here, PAI is assumed to be constant as a seasonal mean value (4.5) because the studied evergreen forest has little seasonal variation in PAI.

Also, for simplification and taking into consideration the studied plot effects, the monthly I_C model applicable for Japanese forest environments can be expressed as (Komatsu et al., 2007):

$$I_C = (4.98 \times 10^{-5} T_D + 0.120)P, \quad (7)$$

where T_D is tree density (trees/ha), and I_C and P are the monthly values.

3. Results

3.1. Environmental and sap flow data

Daily environmental data for the study period are shown in Fig. 1. Maximum T_a reached 35 °C between late July and mid September in 2007. Minimum T_a was –5 °C in mid February, 2008. T_a , and therefore vapor pressure deficit (D ; kPa) showed a seasonal variation. D and daily total R_s were low from mid-June to mid-July in both 2007 and 2008 due to the regular rainy season in Japan. It should be noted that there was an appreciable difference in soil moisture conditions among UP, LP and SP. Both peaks and troughs of θ_{0-50} variations were always in the order SP > LP > UP throughout the studied period because of each plot's soil porosity. Soil water retention curves suggest that the frequency distributions

of soil pore size in LP is significantly higher in the large pore-size region, while those in UP and SP are evenly distributed with a low (negative high) Ψ at air entry (data not shown). This resulted in much lower water extraction Ψ , and thus much lower Ψ in UP and SP during dry spells despite similar range of θ_{0-50} variations among the plots.

The data show that daily J_s and E_{UC} were the largest in the SP and the LP, respectively (Fig. 2a and b). Responses of the daily J_s and E_{UC} to D and R_s patterns and to their seasonal variations were evident. As expected from previous work (Kumagai et al., 2008), J_s (and thus, E_{UC}) did not respond to soil moisture depletions. In particular, water was not limiting to the E despite the frequent strong droughts in 2007 (see Fig. 1).

3.2. Examination of environmental controls on J_s

Given that D and R_s are the primary drivers of E , we proceed to the examinations of their environmental controls on J_s at diurnal time scale for each season, i.e., A and F: mid growing season, B: early dormant season, C and D: start of the growing season, and E: early growing season (see Fig. 2). The typical cases were derived from their linearity, i.e., the smallest (Fig. 3b and c) and largest (Fig. 3a and d) coefficients of determination (R^2) between R_s or D and J_s . Hysteresis is evident in the R_s – J_s relationship ($R^2 = 0.53$ – 0.69 and 0.44 – 0.50 in Fig. 3a and c, respectively), while the D – J_s relationship is approximately linear ($R^2 = 0.81$ – 0.89 and 0.94 – 0.95 in Fig. 3b and d, respectively), suggesting that in a day, J_s peaked later than R_s and at the same time as D . Start of an

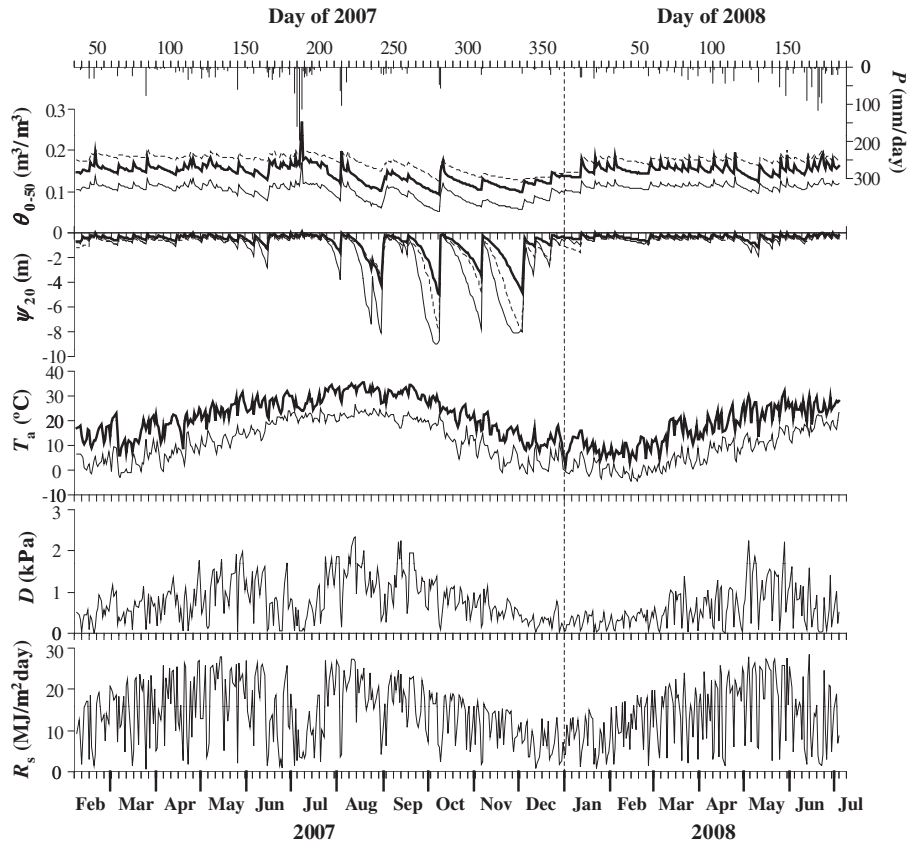


Fig. 1. Yearlong climatic data (DOY 37, 2007 to DOY 185, 2008, February 6, 2007 to July 3, 2008). Reading from the top: daily precipitation (P ; bars, right scale), volumetric soil moisture content in the 0–50 cm soil layer (θ_{0-50}) in the UP (thin solid line), LP (thick solid line), and SP (broken line), soil matric potential at 20 cm depth (Ψ_{20}) in the UP (thin solid line), LP (thick solid line), and SP (broken line), daily maximum (thick line) and minimum (thin line) air temperature (T_a), mean daytime atmospheric humidity deficit (D ; thin line), and daily total solar radiation (R_s ; thin line).

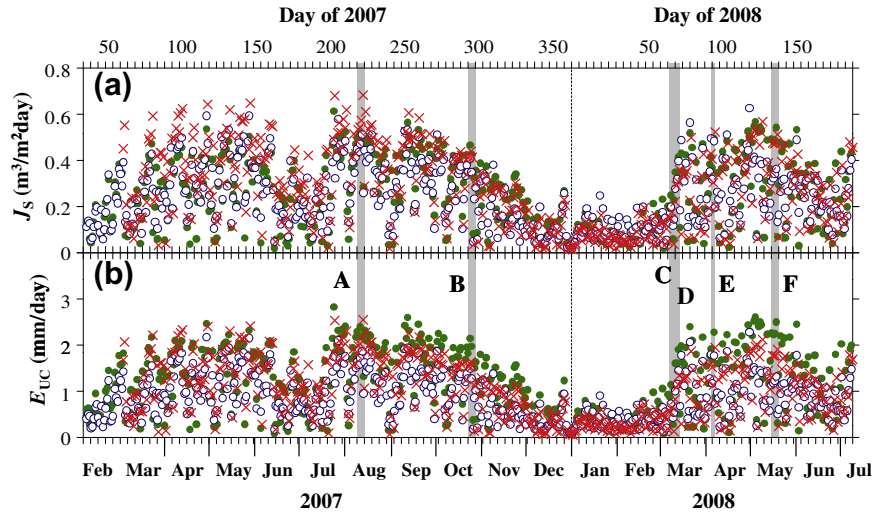


Fig. 2. Seasonal patterns of (a) daily mean stand sap flux density (J_s), and (b) daily upper canopy stand transpiration (E_{UC}) in the UP (open circles), LP (closed circles), and SP (crosses). The gray zones denote the periods used to examine the relationships between diurnal changes in environmental factors and J_s (see Fig. 3).

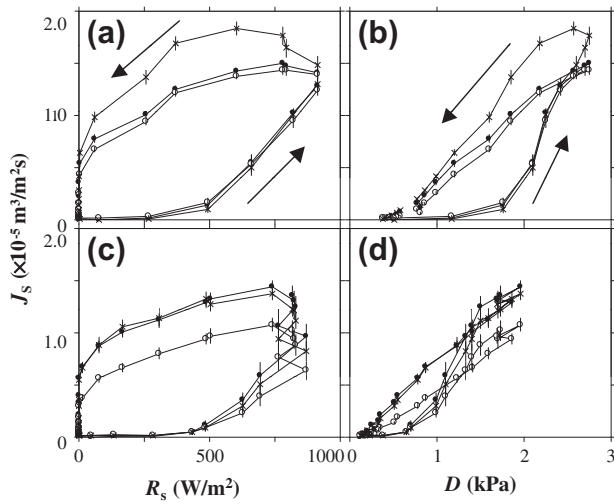


Fig. 3. Relationships between averaged diurnal changes in solar radiation (R_s ; a and c) and vapor pressure deficit (D ; b and d) and stand sap flux density (J_s) in the UP (open circles), LP (closed circles), and SP (crosses). (a and b) Represent period A in August (DOY 220–224), 2007, and (c and d) represent period F in May (DOY 133–138), 2008 (see Fig. 2). Vertical bars represent one standard deviation (SD) of J_s during the sampled periods. The SD of R_s and D were not shown because of their small values.

increase/decrease in J_s in response to increase/ decrease in D and R_s were consistent between the three plots.

Information on what factors in UP, LP and SP impact J_s would be useful when extrapolating larger-scale E from J_s estimated in single and partial plots (Kumagai et al., 2007). Thus, considering Fig. 2a, we compared J_s in LP and UP (Fig. 4a) and SP (Fig. 4b) in each studied period “growing season” DOY 96–322, 2007 and DOY 69–190, 2008 and “winter” DOY 38–95, 2007 and DOY 323, 2007 to DOY 68, 2008, when the minimum T_a was below 0 °C (see Fig. 1). According to a previous study (Kumagai et al., 2008), J_s was clearly much higher in UP than in LP in the winter of 2005. However, such a phenomenon has not been observed since 2006 (data not shown). Using linear regressions with their intercepts forced to be zero, the J_s including values for LP for both winter and the growing season were highly correlated with those in UP ($R^2 = 0.77$; slope equal 0.90) and in SP ($R^2 = 0.88$; slope equal 1.09). The difference between LP and UP was not significantly different from zero (paired

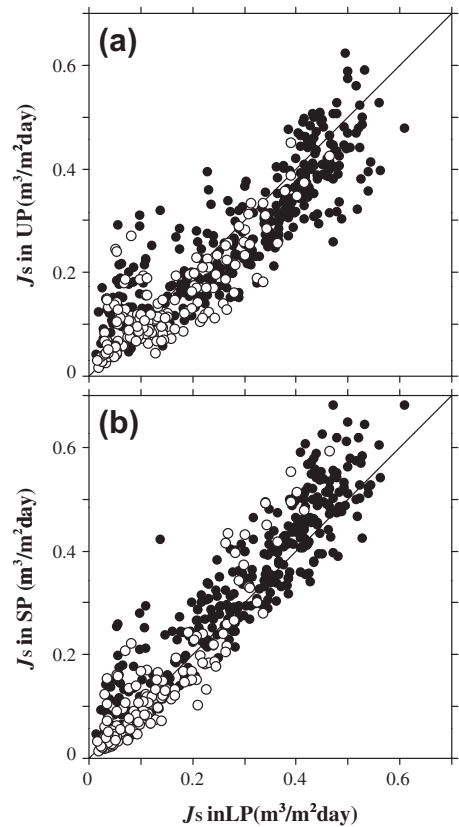


Fig. 4. Comparison between the mean stand sap flux densities (J_s) in the UP and LP (a) and SP and LP (b) during DOY 96–322, 2007 and DOY 69–190, 2008 (growing season; closed circles), and DOY 38–95, 2007 and DOY 323, 2007 to DOY 68, 2008 (winter; open circles). A 1:1 line is also shown.

t -test, $p = 0.14$), while J_s in SP was significantly higher than in LP ($p < 0.01$).

3.3. Evapotranspiration estimations

Fig. 5 compares individual tree water use (T_r) in SP, UP and LP. Maximum T_r in SP, UP and LP reached approximately 25, 20 and

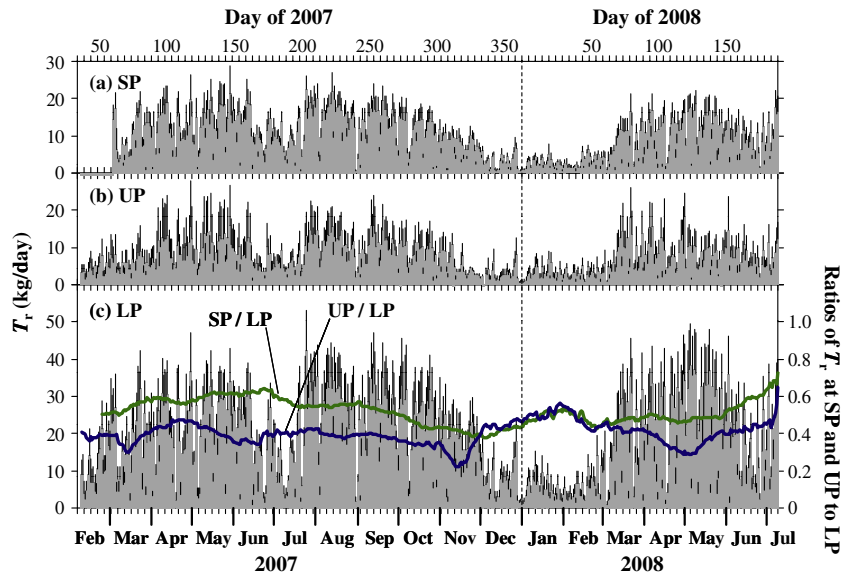


Fig. 5. Daily mean water use of individual trees (T_r ; gray bars) in the SP (a), UP (b) and LP (c). Vertical black bars represent one standard deviation. Ratios of T_r at SP and UP to LP, smoothed by a 20-day running average, are also shown in (c).

45 kg day⁻¹, respectively. Ratios of T_r at SP and UP to LP were relatively constant at 0.6 and 0.4, respectively in the growing season, becoming almost equal (~ 0.5) in the winter (Fig. 5c). Considering that the J_s in the three plots was similar (Fig. 4) and that tree size was much larger in LP than in UP and SP ($SP \geq UP$) (Table 1), it is evident that T_r was correlated to tree size, which depended on its slope position in the watershed.

A more detailed examination of the potential for forest water use management in this watershed needs to address which parameter is the strongest determinant of water use. Assuming that the error in $E_{UC,T}$ ($\delta E_{UC,T}$) is associated with those in J_s and $A_{S,stand}$ for each plot ($\delta J_{S,i}$ and $\delta A_{S,i}$, respectively, where i denotes a plot, i.e., UP, SP and LP), using Eqs. (1) and (2) and considering only the first-order terms in the total derivative expansions results in (e.g., Juang et al., 2007):

$$\begin{aligned} \delta E_{UC,T} &= \sum \left(\frac{\partial E_{UC,T}}{\partial J_{S,i}} \delta J_{S,i} \right) + \sum \left(\frac{\partial E_{UC,T}}{\partial A_{S,i}} \delta A_{S,i} \right) \\ &= \sum \left(\frac{A_{S,i}}{A_{G,T}} \delta J_{S,i} \right) + \sum \left(\frac{J_{S,i}}{A_{G,T}} \delta A_{S,i} \right) \end{aligned} \quad (8)$$

We constructed three types of experimental cases examining $\delta E_{UC,T}$ caused by errors in estimating J_s and $A_{S,stand}$ for each plot in the watershed. Case 1 uses term I in Eq. (8), and computes J_s in UP and SP being equal to the value in LP but retains the observed $A_{S,stand}$ for each plot. Cases 2 and 3 use term II in Eq. (8), and compute $A_{S,stand}$ in UP and SP being equal to the value in LP and using allometric relationship obtained in LP, respectively, but retain the observed J_s for each plot. The values of $\delta E_{UC,T}$ for all cases tend to be small in the winter (Fig. 6). On the other hand, the absolute values of $\delta E_{UC,T}$ for Cases 2 and 3 become higher in the growing season. Annual total $\delta E_{UC,T}$ were -5.1 , 116.9 , and -69.4 mm for Cases 1, 2, and 3, respectively.

Estimations of ET and its components, i.e., E_{UC} and E_{SC} , and I_C , are described in Fig. 7. It is interesting to note that the E_{UC} in SP was almost the same as $E_{UC,T}$ (Fig. 7), probably because $A_{S,stand}$ is the most determinant factor for the stand water use (see Fig. 6) and $A_{S,stand}$ in SP is representative of the three plots. Although there was the limitation for comparison between E_{UC} and E_{SC} estimates because of their different scaling procedure, we delineated

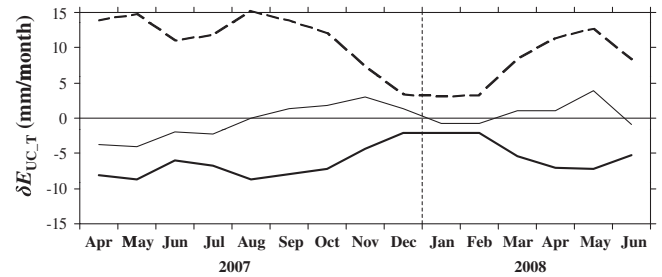


Fig. 6. The errors in monthly total upper canopy stand transpiration over the watershed ($\delta E_{UC,T}$) in Case 1 (thin solid line: in which J_s in UP and SP are equal to J_s in LP), Case 2 (broken line: in which $A_{S,stand}$ in UP and SP are equal to $A_{S,stand}$ in LP), and Case 3 (thick solid line: in which $A_{S,stand}$ in UP and SP are estimated using the allometric relationship obtained in LP).

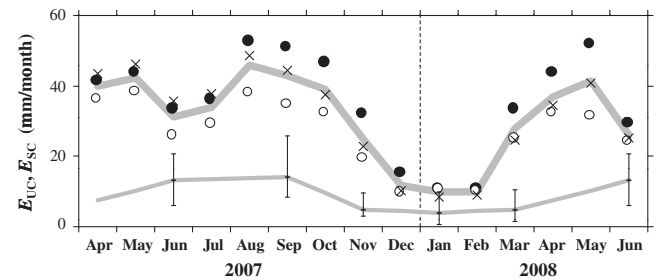


Fig. 7. Monthly transpiration from upper canopy (E_{UC} : UP (open circles), SP (crosses) and LP (closed circles), and total value over the watershed (thick gray line) and sub-canopy (E_{SC} : thin gray line). Top and bottom of the vertical bar represent maximum and minimum values, respectively.

the E_{SC} estimates at one plot but with the individual's E variations in Fig. 7. Note that the ratio of E_{SC} to E_{UC} became larger when E_{UC} was low.

Monthly I_C data were examined from two experimental plots. The linear regression equations fitted to the relationship between incident P in a single storm event and throughfall (TF) and stemflow (SF) were derived from the measurements, and thus we could obtain the P -TF and P -SF equations. The equations showed strong correlations between P and TF and SF, respectively ($R^2 \approx 0.95$). As

one method to estimate I_c , we calculated TF and SF values from the P -TF and P -SF equations, respectively, by inputting P in a single storm event, and subtracting both the TF and SF from the P . This resulted in I_c estimated at each single rainfall event (namely, $I_{c,eq}$). The $I_{c,eq}$ and I_c calculated by subtracting the measured stand TF and SF from gross P for each rainfall event were supposed to be compatible. However, it was found that at one plot, there was a large discrepancy between them, suggesting that the values observed there were unreliable. Therefore, we adopted observed values at the other plot as actual I_c for the studied watershed (Fig. 8).

The difference in I_c between plots estimated using the Komatsu et al. (2007) model (Eq. (7)), which considers the effect of stand variation in tree density, was small. This estimated I_c for UP and the $I_{c,eq}$ were almost the same because Eq. (7) with tree density at UP happened to be able to represent the $I_{c,eq}$ for the experimental plot (Fig. 8). The I_c values by Eq. (7) did not significantly differ from the value estimated by the Kondo et al. (1992) model (Eq. (3)) except for the months with large amounts of precipitation, i.e., the Japanese rainy season (Fig. 8). For example, the I_c in July 2007 and June 2008 was estimated to be more than 100 mm by Eq. (7). Surprisingly, although Eq. (7) was built for estimations of the annual value (see Komatsu et al., 2007), the modeled values showed a good fit to the observed values (Fig. 8). It should be notable that Eq. (3) was built based on the radiative energy balance on the vegetation surface. Thus, for the I_c estimation in heavy rainfall conditions such as in July 2007 and June 2008 in Fig. 8, other factors like active evaporation from the surface of splashes caused by the heavy rainfall should be taken into account (see Murakami, 2006).

Monthly ratios of I_c to P (I_c/P) were very conservative (around 0.2), irrespective of rainfall amounts (Fig. 9). Also, values of ET (ET/P) were somewhat constant (around 0.5), although they tended to be lower during abundant and much higher during scarce rainfall conditions (Fig. 9). When monthly P was low, E_{UC} contributed to ET/P . When P was high, E_{UC} was reduced and I_c much contributed to ET/P because I_c/P is a conservative process. These might result in somewhat constant monthly ET/P . Annual total E_{UC} , E_{SC} , I_c , and ET were 359.3, 126.9, 425.2, and 911.4 mm, respectively.

3.4. Investigation of the annual evapotranspiration throughout Japan

Zhang et al. (2001) proposed a simple annual ET model as a function of P ; this model is applicable throughout the world, but generally cannot be applied to Japanese forest environments (Komatsu et al., 2008b). This is because the equilibrium evaporation (E_{eq}) is a more important factor than P in determining ET in Japan, owing to $P \gg E_{eq}$ (Komatsu et al., 2008b). Furthermore, the E_{eq} value assumed by Zhang et al. (2001) is too high for temperate regions including Japan (Komatsu et al., 2012). The E_{eq} strongly

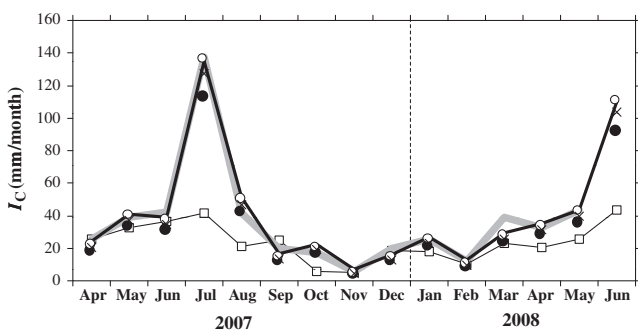


Fig. 8. Monthly canopy interception (I_c) estimated from observations (thick gray line), by subtraction of both P -throughfall and P -stemflow linear regression equations from P (thick solid line), using Eq. (7) for UP (open circles), SP (crosses), and LP (closed circles), and using Eq. (3) for the whole watershed (squares).

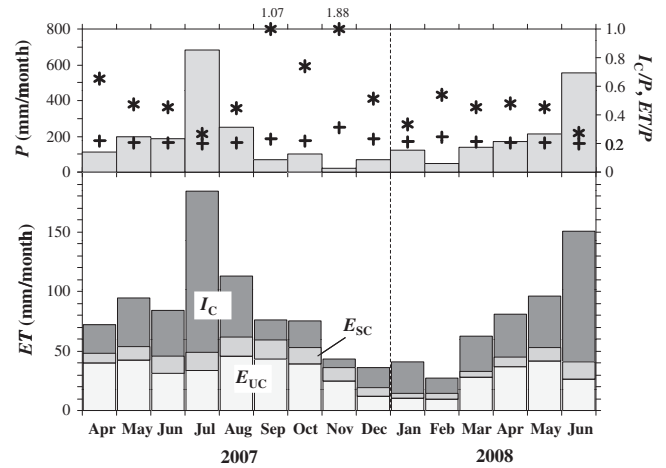


Fig. 9. Upper panel: monthly precipitation (P ; bars) and ratios of canopy interception (I_c) and evapotranspiration (ET) to P (I_c/P : crosses, and ET/P : asterisks, respectively). Bottom panel: summary of monthly ET components.

correlates to T_a , and thus, Komatsu et al. (2008b) formulated a simple annual ET model as a function of annual mean T_a , i.e., ET (mm/year) = $31.4 T_a$ ($^{\circ}C$) + 376, using water balance data ($ET = P - Q$, in which Q is runoff) from 43 watersheds throughout Japan ($R^2 = 0.38$) (Fig. 10). Plotting the value in this study ($15.3^{\circ}C$, 911.4 mm) in Fig. 10a reveals validity of the ET estimated from the forest use components estimations and also practicality of the model of Komatsu et al.

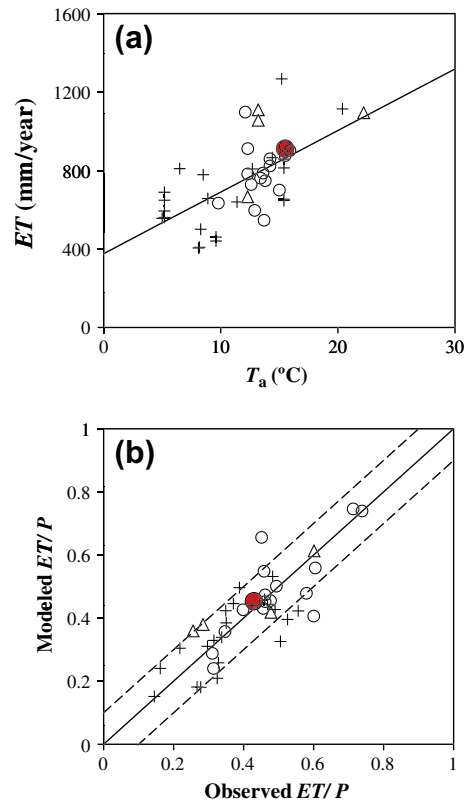


Fig. 10. (a) Relationship between annual mean air temperature (T_a) and annual evapotranspiration (ET) across Japan. Solid line denotes Komatsu et al. (2008b) model, i.e., $ET = 31.4T_a + 376$. (b) Relationship between observed and modeled ET relative to precipitation (ET/P). Solid line and broken lines denote a 1:1 line and 10% estimation error of ET/P , respectively. Forest types: this study (conifer: closed circle), conifers (open circles), hardwoods (triangles), and mix (crosses).

For reference, annual water losses ($P - Q$) estimated from water balance data in the studied and a neighboring watershed (a 3.69 ha coniferous plantation, 160–250 m a.s.l.) were 1332 mm (an average over 2004–2008) and 897 mm (an average over 2000–2008), respectively (Shimizu et al., submitted for publication). Note that while the $P - Q$ value from the studied watershed cannot be adopted as the ET estimate because it was an outlier, the value from the neighboring watershed was on the theoretical line (Fig. 10a). Furthermore, the annual ET estimated using the eddy water vapor flux from the south bank of the studied watershed, occupied mainly with relatively productive Japanese cedar, was 862.6 mm (cf. ~ 650 mm without consideration of the energy imbalance ratio) in 2007. Although there were inconsistencies between monthly ET estimated from the eddy covariance and the water use component measurements in July–September, the eddy ET was approximately on the theoretical line in Fig. 10a (Shimizu et al., submitted for publication). These water balance and eddy flux data validate the ET estimation and also its components in this study.

In Japan, $\sim 10\%$ error in P observation is inevitable for any watershed, and year-to-year variation in Q is mainly caused by the P variation (Komatsu et al., 2007). Thus, it is instructive to examine the relationship between observed and modeled ET/P , resulting in the insignificant difference (paired t -test, $p = 0.51$) (Fig. 10b). The mean error of ET/P estimates was 0.06, indicating that the ET estimates using the model resulted in an error of $\sim 6\%$ relative to P . Most samples including this study's value satisfied the $\ll 10\%$ error in the modeled ET/P . Overall, the annual ET in the studied watershed is located in the upper value zone for Japan (Fig. 10a), and can be well explained by the annual amount of P .

4. Discussion and conclusions

4.1. Determinant factor of the watershed-scale upper canopy stand transpiration

In previous studies (Kumagai et al., 2007, 2008), we discovered a similarity in mean stand sap flux density (J_s) between upper (UP) and lower (LP) plot positions along a slope. The similarity was expected to allow us to extrapolate to the watershed-scale upper canopy stand transpiration (E_{UC}) based on J_s estimated from xylem sap flux density (F_d) measured in a stand in the watershed. In this study, we added a stand plot on a south-facing slope (SP), in an expectation that the watershed-scale E_{UC} ($E_{UC,T}$) will be affected.

The implications of the findings in Fig. 3 are that the differences in the environmental factors, especially water pressure deficit and solar radiation, between plot positions with different slope elevations and aspects had little effect on each plot transpiration (E) in the studied watershed; this is despite some reports about little or large impacts of slope positions (e.g., Bren, 1997; Tromp-van Meerveld and McDonnell, 2006; Kumagai et al., 2007, 2008) and aspects (e.g., Tajchman et al., 1988, 1997; Munro and Huang, 1997) on E in a forest stand. This might be attributed to a lower stomatal response of the studied species, *C. japonica*, to atmospheric evaporative demand and soil moisture deficit (Kumagai et al., 2008), and also means that the climatic variables measured at the canopy tower were representative in the studied watershed.

The statistical analyses using Fig. 4 revealed that overall, J_s measured in a partial stand could be a reasonable estimate for other stands in the watershed, and for watershed-scale estimates of E ; predicting J_s from F_d measurements in a partial stand, e.g., in only LP, would be practical. Here, there was no systematic relationship between F_d and individual tree sapwood area (A_{S_tree}) and tree-to-tree variations in F_d were independent on variations in A_{S_tree} and tree size. As many studies suggest (e.g., Ryan and Yoder, 1997),

the effect of tree height (via the slope position in this study) on the environmental control of individual tree water use (T_r) (see Fig. 5) can be expected, but in this study we did not find such an effect. It should be noted that the greater E_{UC} reflected a larger total sapwood area per ground area of the stand (A_{S_stand}/A_G) in LP, implying that A_{S_stand}/A_G was a strong determinant of water use in this forest watershed (e.g., Dunn and Connor, 1993; Vertessy et al., 1995, 1997; Ewers et al., 1999; Roberts et al., 2001): the previous studies' idea. In addition, in the present study, it was shown that for the $E_{UC,T}$ estimation, the error in the estimation of total sapwood area of the stand (A_{S_stand}) was much more critical than that in the J_s estimation (Fig. 6). Again, the majority implied that quantifying A_{S_stand} is important for understanding the plot-scale E (Adelman et al., 2008; Loranty et al., 2008) and the difference in E_{UC} between the three plots in this study was mainly determined by the A_{S_stand}/A_G of each plot, which was affected by each slope position, despite some importance of tree-to-tree variation in F_d when estimating T_r (Ford et al., 2004).

4.2. Watershed evapotranspiration and its component

Using a combination of observations and modeling, we obtained reliable estimations of the sub-canopy vegetation E (E_{SC}) and canopy interception (I_c) and therefore, yearly variations in the watershed evapotranspiration (ET) and its components; to our knowledge, reliable data for a Japanese forest environment had been lacking.

Previous studies have suggested that, in forests, ET is a conservative process because differences in forest stand status mainly affect partitioning of ET components but not its magnitude (Roberts, 1983; Oren et al., 1998; Delzon and Loustau, 2005; Kosugi and Katsuyama, 2007). There may emerge a compensation for the differences among the ET components. For example, the contribution of E_{SC} to the whole transpiration, i.e., $E_{SC} + E_{UC}$, became larger when E_{UC} decreased (Fig. 7) probably because in the wintertime, incident light could penetrate through the canopy with its reduced LAI and compared with the upper canopy species, sub-canopy species can continue their active productivity (e.g., Miyazawa and Kikuzawa, 2006).

The findings in Fig. 9 seem to support the earlier studies on the conservative process: very conservative I_c/P (where P is precipitation) throughout the year, significant contribution of I_c/P to ET/P on the heavy rainfall condition, and increase/decrease in I_c and E_{SC} when E_{UC} decreases/increases, to retain somewhat constant monthly ET/P for each of growing season and winter. However, it should be noted that in this study, such conservative ET/P were violated under drought conditions (Fig. 9).

On a longer time scale, Kosugi and Katsuyama (2007) reported an invariability of annual Japanese cypress forest ET for 33 years despite tree growth, succession, occasional cutting and natural disturbances. Also, more spatially, Komatsu et al. (2008b) suggested that in Japan, year-to-year variation in runoff from forested watersheds (Q) is caused mainly by variation in precipitation (P), and thus, year-to-year variation in ET ($=P - Q$) is unaltered. Roberts (1983) claimed that variations in soil moisture have negligible effects on transpiration (E) rates in most circumstances. Although his results were based on site-to-site comparisons, his theory is applicable to stand-to-stand comparisons within a site.

Finally, it was found that the annual ET estimation from this study can be well reproduced by the Komatsu et al. (2008b) formulation, which is a function of only annual mean air temperature (T_a) (Fig. 10). Komatsu et al. (2008b) observed a strong correlation between T_a and $\Delta/(\Delta + \gamma)$ and a weak one between T_a and R_n/λ (where Δ is the slope of the vapor saturation curve, γ is a psychrometer constant, R_n is net radiation, and λ is the latent heat of water vaporization), resulting in a close correlation between T_a and the equilibrium evaporation ($E_{eq} = \{\Delta/(\Delta + \gamma)\}(R_n/\lambda)$). Thus, they could

build the ET function of T_a with a confirmation that the ET can be represented by E_{eq} . In addition, they showed the ET function is also available when E_{eq} is close to P . The present results (Fig. 10) validated both this ET estimation and Komatsu et al.'s (2008b) theory.

Ecological and natural resource policies are directing forest managers to control water and carbon cycling (Japan Forest Agency, 2011). The basic information about seasonal variations in ET and its components, obtained in this study, is the first step for allowing numerical simulations to diagnose water and carbon dynamics in Japanese forest ecosystems resulting from forest management.

Acknowledgments

The maintenance of the KHEW is supported by the Kyushu Research Center of the Forestry and Forest Products Research Institute (FFPRI) and the National Forests in Kyushu Office. This work was supported by Grants-in-Aid for Scientific Research (Nos. 17380096 and 17510011) from the Ministry of Education, Culture, Sports, Science and Technology, Japan. This study is part of “The Long-Term CO₂ Flux Observation Project (#200303)” supported by the FFPRI. We are grateful to Kyoichi Otsuki for support and Sayaka Aoki for help with fieldwork.

References

- Adelman, J.D., Ewers, B.E., Mackay, D.S., 2008. Use of temporal patterns in vapor pressure deficit to explain spatial autocorrelation dynamics in tree transpiration. *Tree Physiol.* 28, 647–658.
- Baldocchi, D.D., Ryu, Y., 2011. A synthesis of forest evaporation fluxes- from days to years- as measured with eddy covariance. In: Levia, D.F., Carlyle-Moses, D., Tanaka, T. (Eds.), *Forest Hydrology and Biogeochemistry: Synthesis of Past Research and Future Directions*, Ecological Studies, vol. 216. Springer, New York, pp. 101–116.
- Bren, L.J., 1997. Effects of slope vegetation removal on the diurnal variations of a small mountain stream. *Water Resour. Res.* 33, 321–331.
- Clearwater, M.J., Meinzer, F.C., Andrade, J.L., Goldstein, G., Holbrook, M., 1999. Potential errors in measurement of nonuniform sap flow using heat dissipation probes. *Tree Physiol.* 19, 681–687.
- Collatz, G.J., Ball, J.T., Grivet, C., Berry, J.A., 1991. Regulation of stomatal conductance and transpiration: a physiological model of canopy processes. *Agric. For. Meteorol.* 54, 107–136.
- Delzon, S., Loustau, D., 2005. Age-related decline in stand water use: sap flow and transpiration in a pine forest chronosequence. *Agric. For. Meteorol.* 129, 105–119.
- Dunn, G.M., Connor, D.J., 1993. An analysis of sap flow in mountain ash (*Eucalyptus regnans*) forests of different age. *Tree Physiol.* 13, 321–336.
- Escudero, A., Mediavilla, S., 2003. Decline in photosynthetic nitrogen use efficiency with leaf age and nitrogen resorption as determinants of leaf life span. *J. Ecol.* 91, 880–889.
- Ewers, B.E., Oren, R., Albaugh, T.J., Dougherty, P.M., 1999. Carry-over effects of water and nutrient supply on water use of *Pinus taeda*. *Ecol. Appl.* 9, 513–525.
- Farquhar, G.D., von Caemmerer, S., Berry, J.A., 1980. A biochemical model of photosynthetic CO₂ assimilation in leaves of C3 species. *Planta* 149, 78–90.
- Ford, C.R., McGuire, M.A., Mitchell, R.J., Teskey, R.O., 2004. Assessing variation in the radial profile of sap flux density in *Pinus* species and its effect on daily water use. *Tree Physiol.* 24, 241–249.
- Ford, C.R., Hubbard, R.M., Kloeppel, B.D., Vose, J.M., 2007. A comparison of sap flux-based evapotranspiration estimates with catchment-scale water balance. *Agric. For. Meteorol.* 145, 176–185.
- Fujimori, T., 2000. *Living with Forests*. Maruzen, Tokyo (in Japanese).
- Granier, A., 1987. Evaluation of transpiration in a Douglas-fir stand by means of sap flow measurements. *Tree Physiol.* 3, 309–320.
- Hui, D., Wan, S., Sua, B., Katul, G., Monson, R., Luoa, Y., 2004. Gap-filling missing data in eddy covariance measurements using multiple imputation (MI) for annual estimations. *Agric. For. Meteorol.* 121, 93–111.
- Iida, S., Shimizu, T., Kabeya, N., Nobuhiro, T., Tamai, K., Shimizu, A., Ito, E., Ohnuki, Y., Abe, T., Tsuboyama, Y., Chann, S., Keth, N., 2012. Calibration of tipping-bucket flow meters and rain gauges to measure gross rainfall, throughfall, and stemflow applied to data from a Japanese temperate coniferous forest and a Cambodian tropical deciduous forest. *Hydrol. Process.* 26, 2445–2454.
- Japan Forest Agency, 2011. *Annual Report on Forest and Forestry in Japan: Fiscal Year 2011*. The Ministry of Agriculture, Forestry and Fisheries of Japan, Tokyo (in Japanese).
- Juang, J.-Y., Katul, G., Siqueira, M., Stoy, P., Novick, K., 2007. Separating the effects of albedo from eco-physiological changes on surface temperature along a successional chronosequence in the southeastern United States. *Geophys. Res. Lett.* 34, L21408. <http://dx.doi.org/10.1029/2007GL031296>.
- Komatsu, H., Tanaka, N., Kume, T., 2007. Do coniferous forests evaporate more water than broad-leaved forests in Japan? *J. Hydrol.* 336, 361–375.
- Komatsu, H., Kume, T., Otsuki, K., 2008a. The effect of converting a native broad-leaved forest to a coniferous plantation forest on annual water yield: a paired-catchment study in northern Japan. *For. Ecol. Manage.* 255, 880–886.
- Komatsu, H., Maita, E., Otsuki, K., 2008b. A model to estimate annual forest evapotranspiration in Japan from mean annual temperature. *J. Hydrol.* 348, 330–340.
- Komatsu, H., Shinohara, Y., Kume, T., Otsuki, K., 2008c. Relationship between annual rainfall and interception ratio for forests across Japan. *For. Ecol. Manage.* 256, 1189–1197.
- Komatsu, H., Cho, J., Matsumoto, K., Otsuki, K., 2012. Simple modeling of the global variation in annual forest evapotranspiration. *J. Hydrol.* 420–421, 380–390.
- Kondo, J., Watanabe, T., 1992. Studies on the bulk transfer-coefficients over a vegetated surface with a multilayer energy budget model. *J. Atmos. Sci.* 49, 2183–2199.
- Kondo, J., Watanabe, T., Nakazono, M., 1992. Heat budget evaluation of forest evapotranspiration in Japan. *Tenki* 39, 685–695 (in Japanese).
- Kosugi, K., 1994. Three-parameter lognormal distribution model for soil water retention. *Water Resour. Res.* 30, 891–901.
- Kosugi, Y., Katsuyama, M., 2007. Evapotranspiration over a Japanese cypress forest. II. Comparison of the eddy covariance and water budget methods. *J. Hydrol.* 334, 305–311.
- Kubler, H., 1991. Function of spiral grain in trees. *Trees* 5, 125–135.
- Kumagai, T., Aoki, S., Nagasawa, H., Mabuchi, T., Kubota, K., Inoue, S., Utsumi, Y., Otsuki, K., 2005. Effects of tree-to-tree and radial variations on sap flow estimates of transpiration in Japanese cedar. *Agric. For. Meteorol.* 135, 110–116.
- Kumagai, T., Aoki, S., Shimizu, T., Otsuki, K., 2007. Sap flow estimates of stand transpiration at two slope positions in a Japanese cedar forest watershed. *Tree Physiol.* 27, 161–168.
- Kumagai, T., Aoki, S., Shimizu, T., Otsuki, K., 2008. Transpiration and canopy conductance at two slope positions in a Japanese cedar forest watershed. *Agric. For. Meteorol.* 148, 1444–1455.
- Lorant, M.M., Mackay, D.S., Ewers, B.E., Adelman, J.D., Kruger, E.L., 2008. Environmental drivers of spatial variation in whole-tree transpiration in an aspen-dominated upland-to-wetland forest gradient. *Water Resour. Res.* 44, W02441. <http://dx.doi.org/10.1029/2007WR006272>.
- Miyazawa, Y., Kikuzawa, K., 2006. Physiological basis of seasonal trend in leaf photosynthesis of five evergreen broad-leaved species in a temperate deciduous forest. *Tree Physiol.* 26, 249–256.
- Miyazawa, Y., Otsuki, K., 2010. Comparison of sapling-level daily light capture and carbon gain between a temperate deciduous and a co-occurring evergreen tree species in the growing season and in winter. *Funct. Plant Biol.* 37, 215–222.
- Munro, D.S., Huang, L.J., 1997. Rainfall, evaporation and runoff responses to hillslope aspect in the Shenchong Basin. *Catena* 29, 131–144.
- Murakami, S., 2006. A proposal for a new forest canopy interception mechanism: splash droplet evaporation. *J. Hydrol.* 319, 72–82.
- Nakada, R., Fujisawa, Y., Hirakawa, Y., 1999. Soft X-ray observation of water distribution in the stem of *Cryptomeria japonica* D. Don I: general description of water distribution. *J. Wood Sci.* 45, 188–193.
- Nobuchi, T., Harada, H., 1983. Physiological features of the “white zone” of sugi (*Cryptomeria japonica* D. Don) -cytological structure and moisture content. *Mokuzai Gakkaishi* 29, 824–832.
- Oren, R., Ewers, B.E., Todd, P., Phillips, N., Katul, G., 1998. Water balance delineates the soil layer in which moisture affects canopy conductance. *Ecol. Appl.* 8, 990–1002.
- Oren, R., Phillips, N., Ewers, B.E., Pataki, D.E., Megonigal, J.P., 1999. Sap-flux-scaled transpiration responses to light, vapor pressure deficit, and leaf area reduction in a flooded *Taxodium distichum* forest. *Tree Physiol.* 19, 337–347.
- Pataki, D.E., Oren, R., 2003. Species differences in stomatal control of water loss at the canopy scale in a mature bottomland deciduous forest. *Adv. Water Res.* 26, 1267–1278.
- Pearcy, R.W., Yang, W., 1996. A three-dimensional crown architecture model for assessment of light capture and carbon gain by understory plants. *Oecologia* 108, 1–12.
- Priestley, C.H.B., Taylor, R.J., 1972. On the assessment of surface heat flux and evaporation using large-scale parameters. *Mon. Weather Rev.* 100, 81–92.
- Roberts, J., 1983. Forest transpiration: a conservative hydrological process? *J. Hydrol.* 66, 133–141.
- Roberts, S., Vertessy, R., Grayson, R., 2001. Transpiration from *Eucalyptus sieberi* (L. Johnson) forests of different age. *For. Ecol. Manage.* 143, 153–161.
- Ryan, M.G., Yoder, B.J., 1997. Hydraulic limits to tree height and tree growth: what keeps trees from growing beyond a certain height. *Bioscience* 47, 235–242.
- Sawano, S., Komatsu, H., Suzuki, M., 2005. Differences in annual precipitation amounts between forested area, agricultural area, and urban area in Japan. *J. Jpn. Soc. Hydrol. Water Resour.* 18, 435–440 (in Japanese with English summary).
- Schäfer, K.V.R., Oren, R., Lai, C.-T., Katul, G.G., 2002. Hydrologic balance in an intact temperate forest ecosystem under ambient and elevated atmospheric CO₂ concentration. *Glob. Change Biol.* 8, 895–911.
- Shimizu T., Kumagai T., Kobayashi M., Tamai K., Iida S., Kabeya N., Ikawa R., Tateishi M., Miyazawa, Y., and Shimizu A., Estimation of annual forest evapotranspiration from a coniferous plantation watershed in Japan (2): Comparison of eddy covariance, water budget and sap-flow plus interception loss, *J. Hydrol.* 2013, (submitted for publication).

- Tajchman, S.J., Harris, M.H., Townsend, E.C., 1988. Variability of the radiative index of dryness in an Appalachian watershed. *Agric. For. Meteorol.* 42, 199–207.
- Tajchman, S.J., Fu, H., Kochenderfer, J.N., 1997. Water and energy balance of a forested Appalachian watershed. *Agric. For. Meteorol.* 84, 61–68.
- Tromp-van Meerveld, H.J., McDonnell, J.J., 2006. On the interrelationships between topography, soil depth, soil moisture, transpiration rates and species distribution at the hillslope scale. *Adv. Water Res.* 29, 293–310.
- Vertessy, R.A., Benyon, R.G., O'Sullivan, S.K., Gribben, P.R., 1995. Relationships between stem diameter, sapwood area, leaf area and transpiration in a young mountain ash forest. *Tree Physiol.* 15, 559–567.
- Vertessy, R.A., Hatton, T.J., Reece, P., O'Sullivan, S.K., Benyon, R.G., 1997. Estimating stand water use of large mountain ash trees and validation of the sap flow measurement technique. *Tree Physiol.* 17, 747–756.
- Wilson, K.B., Hanson, P.J., Mulholland, P.J., Baldocchi, D.D., Wullschleger, S.D., 2001. A comparison of methods for determining forest evapotranspiration and its components: sap-flow, soil water budget, eddy covariance and catchment water balance. *Agric. For. Meteorol.* 106, 153–168.
- Wullschleger, S.D., Hanson, P.J., Todd, D.E., 2001. Transpiration from a multi-species deciduous forest as estimated by xylem sap flow techniques. *For. Ecol. Manage.* 143, 205–213.
- Zhang, I., Dawes, W.R., Walker, G.R., 2001. Response of mean annual evapotranspiration to vegetation changes at catchment scale. *Water Resour. Res.* 37, 701–708.